

# Reanalysis of the ionospheric total electron content anomalies around the 2011 Tohoku-Oki and 2016 Kumamoto earthquakes: Lack of a clear precursor of large earthquakes

R. Ikuta<sup>1</sup>, R. Oba<sup>1</sup>, D. Kiguchi<sup>1</sup> and T. Hisada<sup>2</sup>

<sup>1</sup> Faculty of Science, Shizuoka University

<sup>2</sup> Graduate School of Integrated Science and Technology, Shizuoka University

## Key Points:

- Preseismic anomalies detected by correlation analysis by Iwata & Umeno (2016) is not significant compared with that on non-earthquake days.
- Anomalous area rate proposed as precursor in Iwata&Umeno (2017) isn't significant and not applicable to their previous Iwata&Umeno (2016).
- Propagation velocity of TEC anomaly proposed by Iwata & Umeno (2017) is not significant as well.

## Abstract:

We investigate the veracity of the reports by Iwata & Umeno (2016, doi:10.1002/2016JA023036) and Iwata & Umeno (2017, doi:10.1002/2017JA023921), both of which claimed that the observed perturbations in GNSS-based ionospheric total electron content (TEC) could serve as a "precursor" of large earthquakes based on correlation analysis. Iwata & Umeno (2016) defined a spatial correlation of residuals between the observed and predicted TEC time series. They reported that the correlation value is significantly larger before large earthquakes than those observed during non-earthquake periods. Iwata & Umeno (2017), who applied the same method to other large earthquake, claimed that the preseismic ionospheric disturbances can be distinguished from other non-earthquake phenomena based on the small percentage of area where the correlation value exceeds the criterion. They also claimed that the low propagation velocity of the correlation peaks is also a pre-seismic characteristic. Here we tested their claims using a larger dataset. As a result, these three characteristics they claimed to have captured as evidence of earthquake precursors are not significant being frequently observed during normal (non-earthquake) days. In addition to that, the criteria of Iwata & Umeno (2017) cannot be applied to the large earthquake discussed by Iwata & Umeno (2016), and vice versa. Therefore, we can find no basis for claiming that they detected precursors to the earthquakes. The calculation procedure of the correlation function shows that the value is more of an indicator that amplifies small variations synchronized between nearby stations, like medium-scale traveling ionospheric disturbances rather than earthquake precursors.

## 1. Introduction

Heki (2011) triggered a debate between researchers about existence of precursory change of ionospheric total electron content (TEC) before large earthquakes. He claimed to have found anomalous enhancements in TEC starting ~40 minutes

before large earthquakes. Several researchers pointed out the possibility that he was looking at TEC change due to solar-related sources, rather than earthquakes (Utada & Shimizu, 2014), and others pointed out that changes in TEC could be a methodological artifact (Kamogawa & Kakinami (2013), Masci et al. (2015), and later Eisenbeis & Occhipinti (2021)). Then, Heki and co-authors improved the method and introduced an objective index and threshold for anomaly detection and then claimed that it is unlikely that the anomalies occurred by chance before earthquakes based on the low frequency of solar-related anomalies detected by their threshold (Heki & Enomoto, 2015), although which is still been criticized that the frequency was underestimated (Ikuta et al., 2020; Tozzi et al., 2020). In such a situation, Iwata & Umeno (2016; hereafter I&U16) and Iwata & Umeno (2017; hereafter I&U17) proposed a correlation analysis of TEC time series between Global Navigation Satellite System (GNSS) stations, and claimed to have successfully identified the emergence of precursory TEC anomalies approximately 1 hour before both the 11 March 2011 Mw 9.0 Tohoku-Oki earthquake (I&U16) and 15 April 2016 Mw 7.3 Kumamoto earthquake (I&U17). I&U16 have claimed that they were able to detect precursory TEC changes with high correlation values (up to  $C(T)=25$ ), which are much larger than the upper limit ( $C(T)=5$ ) for non-earthquake days (normal days) they showed, such that these precursory earthquake signals can be distinguished from other signals.  $C(T)$  is described in the next section. In addition to the 2011 Tohoku-Oki earthquake, they detected an anomalous area prior to three of the four studied M7-class earthquakes based on slightly lower correlation values than those determined for the Tohoku-Oki earthquake case. I&U17 applied the same procedure to the TEC time series before the 2016 Kumamoto earthquake, and claimed to have detected a precursory TEC correlation change. They also provided two new indicators for distinguishing precursory TEC anomalies from those of space weather origin: those are “anomalous area rates” and “ $C(T)$  propagation velocities”.

We highlight three problems that arise in the two papers. The first is the degree of inconsistency between the two papers. The characteristics of the earthquake precursor reported in I&U16, which is a remarkably large  $C(T)$  that is five times larger than the maximum correlation values for several non-earthquake days was treated as an unremarkable observation in I&U17 since these values were observed during most of the eight non-earthquake days (Figures 9 and 10 in I&U17). I&U17 adopted a completely different set of criteria from I&U16 and did not check whether or not the TEC anomaly prior to the Tohoku-Oki earthquake in I&U16 met the new criteria or not. The second problem is the lack of data during the non-earthquake days. I&U16 only showed the  $C(T)$  values for one satellite during four non-earthquake days to highlight their low values. However, I&U17 found many days with high  $C(T)$  values, including some that were even higher than that before the Tohoku-Oki earthquake (for example, Figures 4, 5, and 8 in I&U17). It is enough to make us suspect that if more data of non-earthquake days had been examined in I&U16, a larger  $C(T)$  would have been found than that before the Tohoku-Oki earthquake. I&U17

also lacked data analysis of non-earthquake-day  $C(T)$  values to fully validate their new criteria. Although I&U17 analyzed the TEC data for one earthquake day and 12 non-earthquake days, the presented results were deduced using only two satellites during eight non-earthquake days to evaluate the first “anomalous area rate” criterion and only one satellite during three non-earthquake days to evaluate the second “propagation velocities” criterion; these are too few data to be treated statistically. The third problem is the loose criteria and/or lack of quantification in I&U17. They introduced the anomalous area rate criterion based on an idea that the anomalous area is smaller in the case of an earthquake precursor than in the case of a signal of space weather origin. However, their own diagrams (Figures 9 and 10 in I&U17) illustrated that the non-earthquake days possessed comparably small anomalous area rates to that on the earthquake day. I&U17 also showed that the  $C(T)$  peak around the focal area of the Kumamoto earthquake propagated more slowly than seasonal medium-scale traveling ionospheric disturbances (MSTIDs), and defined this as the propagation velocity criterion. However, the velocities they provided as an indicator to distinguish an earthquake precursor from MSTIDs were 65–168 m/s (Figures 14 and 15 in I&U17), which is within the MSTID propagation velocity range (e.g. Hunsucker 1982; Hernandez-Pajares et al. 2006).

Here we examine the correlation method developed by I&U16 and I&U17 by applying it to the days without a large earthquake to evaluate the significance of the reported correlation values, anomalous area rates, and propagation velocities before the Tohoku-Oki and the Kumamoto earthquakes.

### 1. Data Processing

We first calculated the vertical TEC (VTEC) from the Global Navigation Satellite System (GNSS) phase data provided by the geospatial information authority of Japan. We then applied the method proposed by I&U16 to the same dataset they analyzed to ensure that we reproduced their method correctly. Here we provide a brief explanation of the procedure; see Section 4 and Supporting Information for full details. A portion of the VTEC time series is first fitted with a regression curve, which is designed to predict VTEC at a future time. The difference between the observed and predicted VTEC values in the future time is recognized as an anomaly  $X(t)$ . The correlation between  $X(t)$  at a central GNSS station and its surrounding 30 stations are then calculated. The average of the correlations for the 30 pairs is regarded as  $C(T)$ :

$$C(T) = \frac{1}{NM} \sum_{i=1}^M \sum_{j=0}^{N-1} X_i(t + t_{\text{sample}} + j t) X_0(t + t_{\text{sample}} + j t) \quad (1)$$

$$T = t + t_{\text{sample}} + t_{\text{test}},$$

in which  $N$  ( $= 31$ ) is the number of data in the prediction time window  $t_{\text{test}}$  ( $= 15$  minutes),  $t$  ( $= 30$  seconds) is a sampling interval,  $t_{\text{sample}}$  ( $= 120$  minutes) is regression time window (240 samples),  $M$  ( $= 30$ ) is the number of stations, and  $X_i(t)$  is anomaly of  $i$ -th station (0 means the central station). We fit the training data for  $t_{\text{sample}}$  with a septic function to predict the data for the future

$t_{test}$  to compute  $X(t)$ . These functions and parameter sets are the same as those adopted in I&U16. Although I&U16 suggested that they can choose a range of functions and parameters, and presented differences in the resulting  $C(T)$  values between various functions and parameters, they only quantitatively evaluated the significance of their result for this parameter sets.

## 1. Results and discussion

### 3-1. $C(T)$ s in non-earthquake days focused by Iwata & Umeno (2016)

Figure S1 shows calculated  $C(T)$  time series for satellite PRN26, and Kitaibaraki (0214) GNSS station (central station) and its 30 surrounding stations on the day of the 2011 Tohoku-Oki earthquake (day of year (DOY) = DOY70) and four selected non-earthquake days (DOY30, 40, 50, and 60 in 2011). These  $C(T)$  variations are similar to those in figures 1 and 3 of I&U16. The  $C(T)$  variations on the earthquake day are about five times larger than those on the non-earthquake days, as I&U16 claimed. The  $C(T)$  values are not exactly the same but very similar. The discrepancy may be due to small differences in the data analysis, such as the number of available GNSS stations (out of 30), the inter-frequency bias (IFB) station corrections during the VTEC pre-processing, and other items that are not outlined in I&U16. We also apply this  $C(T)$  calculation to additional data to test their claims.

We examine  $C(T)$  time series during these days at the stations not shown in I&U16 to determine if  $C(T)$  is really as small as they reported. We adopt an elevation mask angle of 20 degrees for our  $C(T)$  calculation to suppress any unrealistic  $C(T)$  increases due to large VTEC variation near the horizon including multipath effects. This means that we do not calculate  $C(T)$  if the elevation angle is less than 20 degrees for any part of the 135-min time series of the data. Furthermore, a station is not used as the central station if the 30 surrounding stations do not fall within a 100-km radius of that station.

Figure 1 shows the time series of the maximum  $C(T)$  over Japan. The maximum  $C(T)$  values during these non-earthquake days often exceeds five and sometimes reaches 100. However, I&U16 appeared to ignore these large  $C(T)$  values. The maximum  $C(T)$  was especially large on the day of the earthquake (DOY70: Figure 1a) compared with the other days, but the value on the 04:45–05:45 (UTC) interval, which was focused on in I&U16 to infer the earthquake precursor (Figure S1a), is relatively small whereas the 02:00–4:00 (UTC) interval possessed significantly larger maximum  $C(T)$  values. The large  $C(T)$  during the day of the earthquake (DOY70) might have been due to the relatively high geomagnetic activity, as suggested by the  $K_p$  index provided by the German Research Centre for Geosciences. The averaged geomagnetic activity indices  $K_p$  for the 00:00 to 09:00 (UTC) interval on DOY30, DOY40, DOY50, DOY60 and DOY70 were 0+, 0, 2, 3– and 5, respectively. Although there is not necessarily a clear correlation between the  $K_p$  index and the maximum value of  $C(T)$  (See Figure S4. Large  $C(T)$  peak tends to appear with large  $K_p$ ), at least for DOY70 (the day of the earthquake) when the  $K_p$  index is significantly larger than other days, the

variation of  $C(T)$  is very large. A frequency histogram of the maximum  $C(T)$  for the 02:00–10:00 (UTC) interval during nine non-earthquake days in 2011 (DOY30, DOY31, DOY40, DOY49, DOY50, DOY60, DOY63, DOY72, and DOY73) is shown in Figure 2. The  $C(T)$  values for the non-earthquake days are not necessarily small, as I&U16 claimed. Therefore, our more comprehensive analysis indicates that the precursory  $C(T)$  increase reported by I&U16 with satellite PRN26 at GNSS station 0214 before the 2011 Tohoku-Oki earthquake is not significantly large compared with the  $C(T)$  increases during other periods.

### **3-2. Anomalous area rate and propagation velocities focused by Iwata & Umeno (2017)**

We next test the significance of the anomalous area rate criterion proposed by I&U17. They claimed that the anomalous area rate, which is the percentage of stations with  $C(T)$  above a threshold (20) among all of the GNSS stations, clearly proves that earthquake days and non-earthquake days possess significantly different  $C(T)$  values based on the data for nine days: the earthquake day (15 April 2016) and eight non-earthquake days (1–5 January and 12–14 April 2016). They showed that large  $C(T)$  values occurred within a relatively limited number of stations (~10 %) during the earthquake day, and interpreted that these observations were due to the fact that these earthquake-precursory anomalies occur within a narrower range than those caused by MSTIDs. They claimed that large anomalous area rates were seen on days when MSTIDs were observed. However, small anomalous area rates were not only seen on the earthquake day. For example, small anomalous area rates (<10%) were observed on 12 April, 14 April, and 3 January in Figures 9 and 10 of I&U17 that were comparable with that for the earthquake day. We test their claim based on the  $C(T)$  values that were calculated during the daytime for 12 non-earthquake days (11:15–19:00 local time (LT) for DOY30, DOY31, DOY40, DOY49, DOY50, DOY60, DOY63, DOY72, and DOY73 in 2011, and DOY96, DOY106, and DOY116 in 2016) and during the nighttime for two non-earthquake days (19:15 the day before–5:00 LT for DOY96 and DOY116 in 2016) against the  $C(T)$  peak values. Figure 3a shows the anomalous area rates when the maximum  $C(T)$  value exceeded 20. The anomalous area rates are generally proportional to the maximum  $C(T)$ . We can see that there are many cases where the maximum  $C(T)$  exceeded 30 whereas the anomaly rate was <5% for these 14 non-earthquake periods. The pre-seismic values for the Tohoku-Oki and Kumamoto earthquakes do not appear to be either significant or unique, as they are buried among other values that are observed during non-earthquake periods.

We finally test their claim of the low propagation velocity of the  $C(T)$  peak. The propagation velocities are estimated for the  $C(T)$  peaks discussed above via semblance analysis. Semblance analysis is a method of determining the velocity of a propagating wave using an array of observation stations. We assume that the target wave propagates at a constant velocity, such that the time of the waveform at each station is shifted by the time difference based on the assumed velocity vector, with the shifted waveforms for each station then summed

according to the following semblance equation:

$$, \quad (2)$$

where  $\Delta t$  is the sampling interval [30 s],  $x_i$  and  $y_i$  are east–west and north–south coordinates of the  $i$ -th station in the array with respect to a reference station [m], respectively;  $p$  and  $q$  are the assumed eastward and northward slowness of the propagating wave [s/m];  $K$  is the number of samples in the time series; and  $M$  is the number of stations used to calculate the semblance. Here we define  $K$  as 120 (60 min) and  $M$  as the number of stations located within 200 km of the reference station. Figure 3b shows the estimated propagation velocities of the C(T) peaks. The C(T) propagation velocities observed before the Tohoku-Oki and Kumamoto earthquakes are estimated to be  $0.37 \pm 0.03$  km/s and  $0.11 \pm 0.01$  km/s, respectively. Therefore, the propagation velocity before the 2011 Tohoku-Oki Earthquake is typical of the propagation velocity distribution of the non-earthquake periods, whereas that before the 2016 Kumamoto Earthquake is close to the lower limit of those observed during the non-earthquake periods. However, neither of these suggested earthquake precursor signals possess values that are not seen during the non-earthquake periods. The claim by I&U17 that C(T) only exhibits a prominent feature in the pre-seismic case is therefore incorrect. Previous studies have indicated that the 65–168 m/s pre-seismic C(T) propagation velocity range reported by I&U17 is not abnormally low as MSTID (e.g., Thome, 1964; Hansucker, 1982). For example, Hernández-Pajares et al. (2006) estimated 50–400 m/s MSTID propagation velocities for 400–1200-s period signals observed using the GNSS network.

We can find no evidence that I&U16 and I&U17 have definitively captured the precursors of the two large earthquakes as they claimed, in terms of either the C(T) magnitude, anomalous area ratio, or C(T) propagation velocity.

### 1. Nature of C(T)

Finally, we discuss the nature of C(T) proposed by I&U16 and following papers by Umeno (Iwata & Umeno 2017, Goto et al. 2019). C(T) is inter-station average of the correlation between VTEC anomalies  $X(t)$  of the central and the surrounding 30 stations.  $X(t)$  is the difference between observed and predicted VTEC. During the training period, the VTEC is fitted with a polynomial function, which is somewhat unsuitable for predicting the future. The function sometimes draws a curve that deviates unrealistically from the observed value in the future prediction period, which is resulting from overfitting of small fluctuations that appear in the training period (See Figure S1a and Movie S1). As a result, C(T) should not be an indicator of perturbation of the observed VTEC in the predicted period, but rather an indicator of synchronized small fluctuations among stations in the training period. We can see this in terms of the much larger magnitude of the obtained C(T) than the value expected from the observed VTEC. For example, Heki & Enomoto 2015 detected anomalies by fitting VTEC values over 80 minutes time window with two straight lines with a break at the center of it. They then adopted a positive gradient change of 3.5

TECU/h between the two lines as a threshold for anomaly detection. Assuming that this gradient change of 3.5 TECU/h occurred for all stations in common,  $X_0(t)$  and  $X_i(t)$  in Equation 1 can be approximated as  $3.5j t/3600$ . Substituting these values into Equation 1,  $C(T)$  is only about 0.5 [TECU<sup>2</sup>]. In contrast, the actual  $C(T)$  is up to a few tens and a few hundred in some cases. This discrepancy comes from the fact that the method does not represent variation of VTEC during the prediction period, but rather the anomalous variation of the reference function itself. Somewhat interestingly, the precursory  $C(T)$  variations proposed by their papers (Figures 1 and 10 in I&U16; Figure 2 in I&U17; Figures 2, 3 and 4 in Goto et al. 2019; Figure S2) show a large oscillation with a period of about 15-20 minutes in  $C(T)$ , which is also shown in non-earthquake days (Figure S3). This oscillation period ranges within half of a typical MSTID period between 15-60 min (Hunscker 1982), reflecting the fact that  $C(T)$  folds the negative side of the VTEC sinusoidal variation, thus halving the period. Note that the oscillation period of  $C(T)$  in Figure S3b seems to be longer than that expected from the more frequent curvature change of VTEC in Figure S3a. Seeing how VTEC is fitted in Movie S2, it seems that the septic function cannot adequately trace this short period variation. Therefore, the oscillation period of  $C(T)$  seems to be determined by the constraint of the order of the fitting function and the oscillation period of the VTEC itself.

Contrary to their claim that  $C(T)$  can selectively detect VTEC change of seismic origin, it is an indicator that amplifies small fluctuations synchronized between nearby stations, such as MSTIDs.

### Acknowledgements

We acknowledge Dr. T. Sakai at the Electronic Navigation Research Institute (<https://www.enri.go.jp/>) and the Astronomical Institute, University of Bern (<https://www.aiub.unibe.ch/>), for providing the receiver IFBs and satellite DCBs, respectively. We thank two anonymous reviewers for their critical and constructive comments. All GNSS data were provided by Geospatial Information Authority of Japan (<https://terras.gsi.go.jp/>).

### References

- Eisenbeis, J., & Occhipinti, G. (2021). The TEC enhancement before seismic events is an artifact, *Journal of Geophysical Research: Space Physics*, **126**, e2020JA028733. doi:10.1029/2020JA028733.
- Goto, S.-I., Uchida, R., Igarashi, K., Chen, C.-H., Kao, M., & Umeno, K. (2019). Preseismic ionospheric anomalies detected before the 2016 Taiwan earthquake. *Journal of Geophysical Research: Space Physics*, **124**, 9239–9252. doi:10.1029/2019JA026640.
- Heki, K. (2011), Ionospheric electron enhancement preceding the 2011 Tohoku-Oki earthquake, *Geophysical Research Letters*, **38**, L17312.

- Heki, K. & Enomoto, Y. (2015), Mw dependence of pre-seismic ionospheric electron enhancements, *Journal of Geophysical Research, Space Physics*, **120**, 7006-7020.
- Hernández-Pajares, M., J. M. Juan, and J. Sanz (2006), Medium-scale traveling ionospheric disturbances affecting GPS measurements: Spatial and temporal analysis, *Journal of Geophysical Research; Space Physics*, **111**, A07S11, doi:10.1029/2005JA011474.
- Hunscker, R. D. (1982), Atmospheric gravity waves generated in the high-latitude ionosphere: A review, *Review of Geophysics and Space Physics*, **20**, 2, 239-315  
doi:10.1029/RG020i002p00293
- Ikuta, R., Hisada, T., Karakama, G., & Kuwano, O. (2020). Stochastic evaluation of pre-earthquake TEC enhancements. *Journal of Geophysical Research: Space Physics*, *125*, e2020JA027899.  
doi:10.1029/2020JA027899.
- Iwata, T., and Umeno, K. (2016), Correlation analysis for pre-seismic total electron content anomalies around the 2011 Tohoku-Oki earthquake, *Journal of Geophysical Research; Space Physics*, *121*, 8969–8984, doi:10.1002/2016JA023036.
- Iwata T., and Umeno, K. (2017), Preseismic ionospheric anomalies detected before the 2016 Kumamoto earthquake, *Journal of Geophysical Research; Space Physics*, *122*, 3602–3616, doi:10.1002/2017JA023921.
- Kamogawa, M. & Kakinami, Y. (2013), Is an ionospheric electron enhancement preceding the 2011 Tohoku-oki earthquake a precursor?, *Journal of Geophysical Research; Space Physics*, *118*, 1-4, doi:10.1002/jgra.50118.
- Masci, F., Thomas, J. N., Villani, F., Secan, J. A. & Rivera, N. (2015). On the onset of ionospheric precursors 40 min before strong earthquakes. *Journal of Geophysical Research: Space Physics*, *120*, 1383–1393, doi:10.1002/2014JA020822.
- Thome G. D. (1964), Incoherent scatter observations of traveling ionospheric disturbances, *Journal of Geophysical Research; Space physics*, **69**, 19, 4047-4049
- Tozzi, R., Masci, F., & Pezzopane, M. (2020). A stress test to evaluate the usefulness of Akaike information criterion in short-term earthquake prediction. *Scientific Reports*, **10**(1), 21153, doi:10.1038/s41598-020-77834-0.
- Utada, H., and H. Shimizu (2014), Comment on “Preseismic ionospheric electron enhancements revisited” by K. Heki and Y.

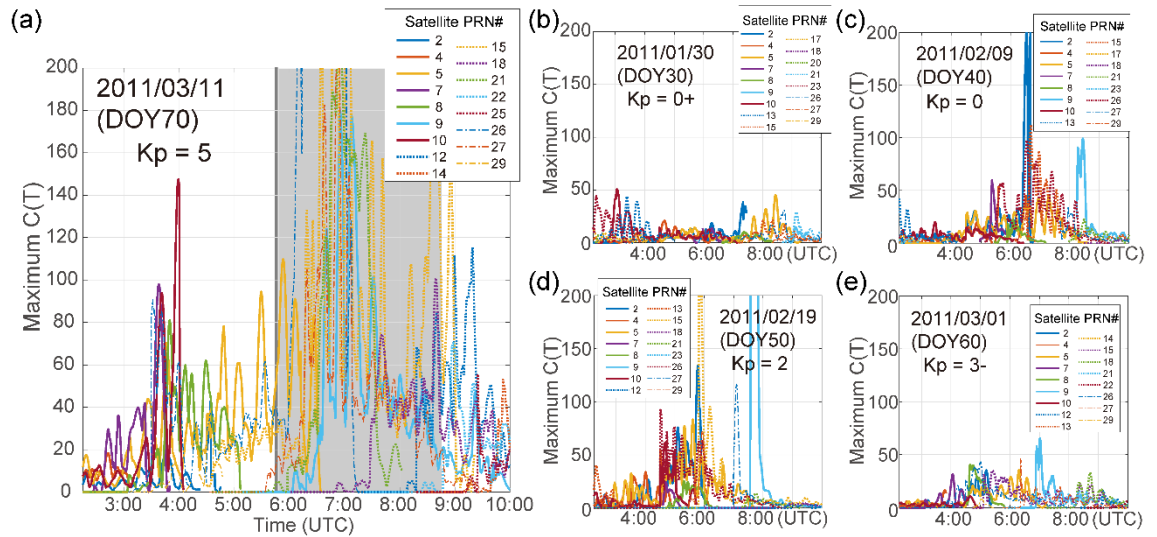


**Figure 1.** Time series of the maximum  $C(T)$  values for each of the satellites and all of the GNSS stations in Japan. (a) The day of the 2011 Tohoku-Oki earthquake (DOY70). The time of the main shock is indicated by the vertical line. The  $C(T)$  values in the shaded period (05:46–08:46 UTC) are not counted in Figure 2 to avoid the post-seismic ionospheric disturbances. (b) Forty days (DOY30), (c) 30 days (DOY40), (d) 20 days (DOY50), and (e) 10 days (DOY60) before the earthquake.

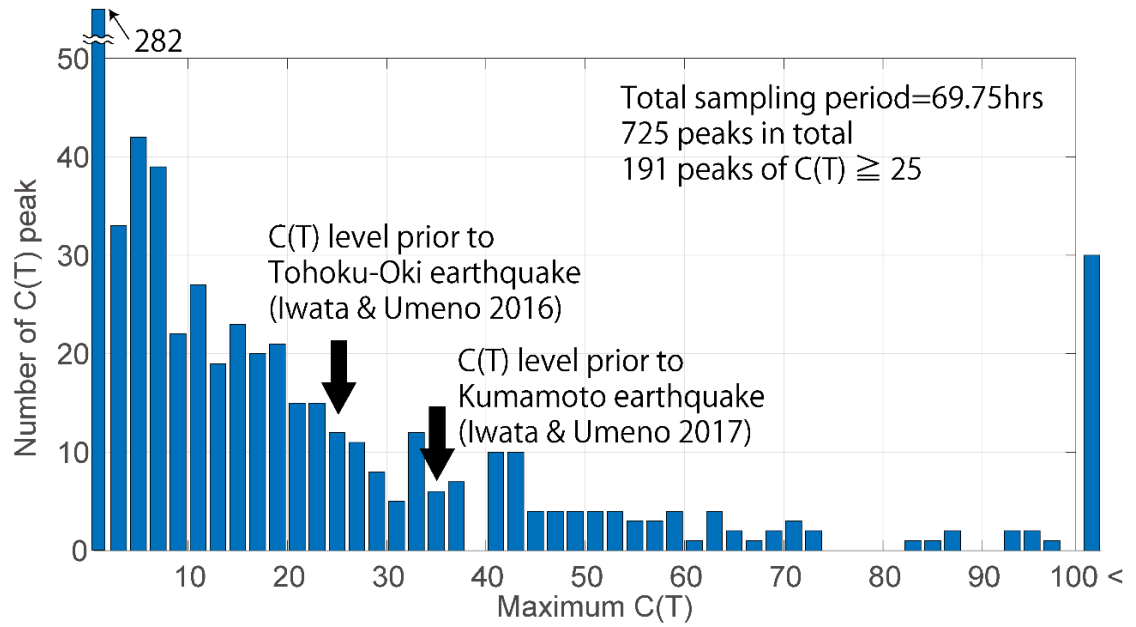


**Figure 2.** Histograms of hourly maximum  $C(T)$  during the 02:15–10:00 (UTC) interval of nine non-earthquake days (DOY30, DOY31, DOY40, DOY49, DOY50, DOY60, DOY63, DOY72, and DOY73 in 2011). Note that the days of Tohoku-Oki and Kumamoto earthquakes are not included in the histogram. The  $C(T)$  levels reported by I&U16 and I&U17 as earthquake precursor are shown by arrows.

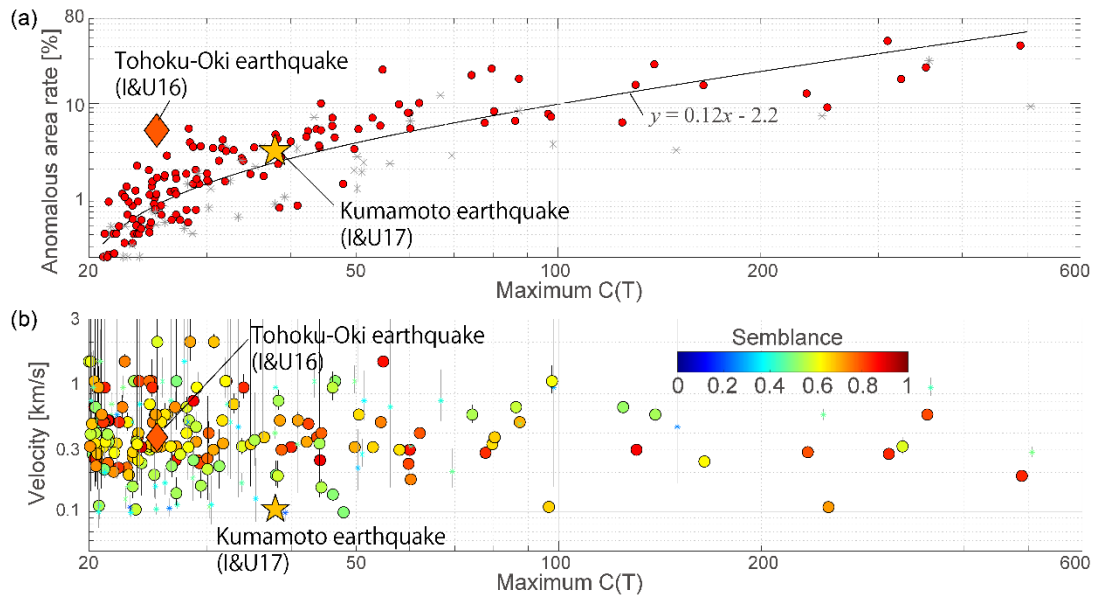


**Figure 3.** Anomalous area rate and propagation velocity of the C(T) peaks for the C(T) values. (a) Anomalous area rate against the C(T) peak value for the 14 non-earthquake periods (See main text). Red circles and asterisks indicate semblance values of  $>0.5$  (more coherent wave) and  $<0.5$  (less coherent), respectively. The diamond marks the value that was calculated at 05:20 UTC using satellite PRN26 and central station 0214 before the 2011 Tohoku-Oki Earthquake (DOY70, 5:46 UTC), which was reported by I&U16. The star corresponds to that before the 2016 Kumamoto Earthquake (DOY106, 16:25 UTC) at 16:09 UTC using satellite PRN17 and central station 0087, which was reported by I&U17. The curvature is the linear trend of the anomalous area rate relative to the C(T) peak, shown for reference. (b) C(T) peak propagation velocities for the peak values. Circles show the values during the same 14 non-earthquake period shown in Figure 3a. The circles are color-coded to show semblance values. The diamond and star represent the two earthquakes as Figure 3a.